Title

Daptomycin Dose-Ranging Evaluation with Single-Dose versus Multidose Ceftriaxone Combinations against Streptococcus mitis/oralis in an Ex Vivo Simulated Endocarditis Vegetation Model.

Journal

Antimicrobial Agents and Chemotherapy, 63(6)

ISSN

0066-4804

Authors

Kebriaei, Razieh
Rice, Seth A
Stamper, Kyle C
et al.

Publication Date

2019-06-01

DOI

10.1128/aac.00386-19

Peer reviewed

AMERICAN SOCIETY FOR MICROBIOLOGY | Antimicrobial Agents and Chemotherapy®

PHARMACOLOGY

Daptomycin Dose-Ranging Evaluation with Single-Dose versus Multidose Ceftriaxone Combinations against *Streptococcus mitis/oralis* in an *Ex Vivo* Simulated Endocarditis Vegetation Model

Razieh Kebriaei,[a] Seth A. Rice,[a] Kyle C. Stamper,[a] Ravin Seepersaud,[e,j] Cristina Garcia-de-la-Maria,[b] Nagendra N. Mishra,[c,i] Jose M. Miro,[b] Cesar A. Arias,[d,g,h] Truc T. Tran,[d] Paul M. Sullam,[e,j] Arnold S. Bayer,[c,i] Michael J. Rybak[a,f]

[a]Anti-Infective Research Laboratory, Eugene Applebaum College of Pharmacy and Health Sciences, Detroit, Michigan, USA
[b]Infectious Diseases Service, Hospital Clinic-Institut d'Investigacions Biomèdiques August Pi i Sunyer (IDIBAPS), University of Barcelona, Barcelona, Spain
[c]LA Biomedical Research Institute, Harbor-UCLA Medical Center, Torrance, California, USA
[d]Center for Antimicrobial Resistance and Microbial Genomic, Division of Infectious Diseases, UTHealth McGovern Medical School, Houston, Texas, USA
[e]University of California, San Francisco, San Francisco, California, USA
[f]School of Medicine, Wayne State University, Detroit, Michigan, USA
[g]Center for Infectious Diseases, UTHealth School of Public Health, Houston, Texas, USA
[h]Molecular Genetics and Antimicrobial Resistance Unit, International Center for Microbial Genomics, Universidad El Bosque, Bogota, Colombia
[i]The Geffen School of Medicine at UCLA, Los Angeles, California, USA
[j]San Francisco VA Medical Center, San Francisco, California, USA

ABSTRACT The viridans group streptococci (VGS) are a heterogeneous group of organisms which are important components of the normal human oral flora. Among the VGS, the *Streptococcus mitis/oralis* subgroup is one of the most common causes of infective endocarditis (IE). Daptomycin (DAP) is a potential alternative therapeutic option for invasive *S. mitis* infections, given high rates of β-lactam resistance and vancomycin tolerance in such strains. However, the ability of these strains to rapidly evolve high-level and durable DAP resistance (DAP-R) is problematic. Recent data suggest that combination DAP-β-lactam therapy circumvents this issue. Human-simulated dose-escalating DAP-alone dose regimens (6, 8, 10, or 12 mg/kg/day times 4 days) versus DAP (6 mg/kg/day) plus ceftriaxone (CRO) (2 g once daily times 4 days or 0.5 g, single dose) were assessed against two prototypical DAP-susceptible (DAP-S) *S. mitis/oralis* strains (SF100 and 351), as measured by a pharmacokinetic/pharmacodynamic (PK/PD) model of simulated endocardial vegetations (SEVs). No DAP-alone regimen was effective, with regrowth of high-level DAP-R isolates observed for both strains over 96-h exposures. Combinations of DAP-CRO with either single- or multidose regimens yielded significant reductions in $\log_{10}$ CFU/g amounts within SEVs for both strains (~6 $\log_{10}$ CFU/g) within 24 h. In addition, no DAP-R strains were detected in either DAP-CRO combination regimens over the 96-h exposure. In contrast to prior *in vitro* studies, no perturbations in two key cardiolipin biosynthetic genes (*cdsA* and *pgsA*) were identified in DAP-R SEV isolates emerging from strain 351, despite defective phospholipid production. The combination of DAP-CRO warrants further investigation for treatment of IE due to *S. mitis/oralis*.

KEYWORDS ceftriaxone, daptomycin, SEVs

The viridans group streptococci (VGS) are important pathogens in invasive diseases, such as infective endocarditis (IE) and intra-abdominal infections (1–3). Among the VGS, the *Streptococcus mitis*/oralis subgroup is a leading cause of IE (3–5). Antibiotic therapy of invasive *S. mitis/oralis* infections is difficult, since a significant proportion of these strains are resistant to β-lactams, including the third-generation cephalosporins,

Citation Kebriaei R, Rice SA, Stamper KC, Seepersaud R, Garcia-de-la-Maria C, Mishra NN, Miro JM, Arias CA, Tran TT, Sullam PM, Bayer AS, Rybak MJ. 2019. Daptomycin dose-ranging evaluation with single-dose versus multidose ceftriaxone combinations against *Streptococcus mitis/oralis* in an *ex vivo* simulated endocarditis vegetation model. Antimicrob Agents Chemother 63:e00386-19. https://doi.org/10.1128/AAC.00386-19.

Address correspondence to Michael J. Rybak, m.rybak@wayne.edu.

Received 22 February 2019
Returned for modification 19 March 2019
Accepted 4 April 2019
Accepted manuscript posted online 8 April 2019
Published 24 May 2019

TABLE 1 MIC values for DAP, CRO, and DAP in the presence of CRO

Strain	MIC (μg/ml)		
	DAP	CRO	DAP-CRO
351	0.5	8	0.25
SF100	0.5	0.125	0.25
Strain pairs[a]			
351/D12T96 A1	0.5/>256		
SF100/D12T96 B2	0.5/>256		

[a]First strain in each pair is the DAP-S parental strain, and the second is the DAP-R strain.

and also exhibit *in vitro* vancomycin tolerance (3, 6–9). The mechanism of β-lactam-resistance in these isolates relates to a reduction of antibiotic affinity to target penicillin-binding proteins (10).

Daptomycin (DAP) has activity against *S. mitis/oralis* and therefore is a potential alternative for treating these infections (11). Although DAP has demonstrated excellent *in vitro* activity against *S. mitis/oralis*, several studies have reported that more than 25% of DAP-susceptible (DAP-S) strains rapidly develop high-level (MICs of >256 μg/ml) and durable DAP resistance (DAP-R) during *in vitro* exposures to DAP; a similar observation has been made *in vivo* in experimental IE (2, 12). The mechanism of DAP-R in *S. mitis/oralis* involves, at least in part, single nucleotide polymorphisms (SNPs) within *cdsA* (a locus encoding an enzyme responsible for catalyzing the first committed step in cardiolipin biosynthesis) and *pgsA*, encoding the enzyme responsible for the synthesis of phosphatidylglycerol (13–15). Such SNPs result in essentially no detectable cardiolipin production (14, 15). Cardiolipin serves a number of biologic functions, especially in cell division; it appears to be a pivotal molecule related to the interaction of DAP with target bacteria via mechanisms that are not fully elucidated but are likely to be associated with localization of anionic phospholipid microdomains in the bacterial cell membrane (16–18).

DAP is a cyclic lipopeptide antibiotic that has been broadly utilized for severe Gram-positive infections, including *Staphylococcus aureus* and enterococci (11). We have previously demonstrated that combinations of DAP plus ceftaroline (CPT) or ceftriaxone (CRO) are synergistic both *in vitro* and in the simulated endocardial vegetation (SEV) model against two well-characterized DAP-S *S. mitis/oralis* parental strains (the penicillin-resistant *S. mitis/oralis* strain, 351, and the penicillin-susceptible strain *S. mitis/oralis* SF100) (19). This model has the advantage of being able to precisely simulate human antibiotic concentrations to replicate therapeutic regimens used to treat specific infections (19–23). In this SEV model, not only did the combination of standard dose DAP (6 mg/kg) plus either CPT or CRO significantly reduce SEV CFU, but it also prevented the emergence of DAP-R over a 96-h exposure period in both strains (2, 24). In contrast, standard dose DAP-alone therapy was associated with inferior bactericidal effects and was unable to prevent the emergence of high-level DAP-R (19).

The aims of the current study utilizing the SEV model were (i) to determine whether escalating DAP-alone dose regimens (6, 8, 10, and 12 mg/kg), as currently commonly used in clinical practice (25, 26), could improve killing as well as prevent the emergence of DAP-R among *S. mitis/oralis* strains and (ii) to delineate whether short-term (single-dose) CRO combination therapy would be as effective as longer term (4 days) strategies as measured by these two outcome metrics.

RESULTS

***In vitro* susceptibility data.** To identify the impact of CRO on the activity of DAP against the *S. mitis/oralis* strains, we determined the MIC values for DAP and CRO alone and in combination. The MICs for each antimicrobial agent alone, as well as the DAP MICs in the presence of CRO at 0.5× MIC, are summarized in Table 1. MIC values for strain pairs are also presented in Table 1. Interestingly, the DAP MICs were reduced by 2-fold in both *S. mitis/oralis* 351 and SF100 strains in the presence of CRO at 0.5× its MIC. These data confirm the impact of CRO on DAP susceptibility. The lowering of the

TABLE 2 PK data for different doses in SEV model

Dose	C_{max} (mg/liter)	AUC_{0-24} (mg · h/liter)	$t_{1/2}$ (h)
DAP 6 mg/kg	93.27 ± 0.51	1,029.19 ± 43.73	7.89 ± 0.19 h
DAP 8 mg/kg	124.82 ± 0.72	1,404.865 ± 7.82	7.93 ± 0.03
DAP 10 mg/kg	143.98 ± 0.35	1,759.41 ± 59.90	8.21 ± 0.11
DAP 12 mg/kg	186 ± 3.32	2,251.99 ± 80.31	7.98 ± 0.08
CRO 2 g/kg	278.9 ± 8.41	3,346.35 ± 108.52	7.88 ± 0.01
CRO 0.5 g/kg	66.75 ± 2.41	756.27 ± 7.45	7.86 ± 0.08

DAP MIC with addition of this β-lactam is consistent with our previous work using other cephalosporins against *S. mitis/oralis* strains (19).

Pharmacokinetics. To humanize the dosing of DAP and CRO, we targeted standard and high-dose DAP (6 and 8, 10, and 12 mg/kg/day, respectively) as well as high-dose (2 g every 24 h [q24h]) and single exposure (500 mg once on day 1) CRO. The average maximum concentration of drug in serum (C_{max}), half-life ($t_{1/2}$), and area under the concentration-time curve from 0 to 24 h (AUC_{0-24}) values for each dose regimen are listed in Table 2.

A high-performance liquid chromatography (HPLC) assay demonstrated intraday coefficients of variation of between 0.48% and 5.13% for all DAP standards. Bioassay tests for CRO levels demonstrated intraday coefficients of variation of between 0.27% and 7.22% for CRO standards. Our data confirm the ability to achieve the targeted pharmacokinetics of DAP and CRO in the SEV model.

Pharmacodynamics. To assess the impact of CRO on the efficacy of DAP as well as the suppression of DAP resistance, we evaluated DAP alone and DAP plus CRO in combination, including a single CRO dose on day one. For strain 351 (Fig. 1), the combination of DAP 6 mg/kg plus CRO (2 g once daily) reduced viability down to the detection limit within 8 h (−Δ 6.046 $\log_{10}$ CFU/g), while the combination of DAP 6 mg/kg plus CRO (single dose at 0.5 g simulation) reached the detection limit in 24 h (−Δ 6.06 $\log_{10}$ CFU/g). CRO alone (2 g) killed to near-detection limits at 32 h (−Δ 5.86 $\log_{10}$ CFU/g), with some regrowth of 0.5 $\log_{10}$ CFU/g at 96 h; however, it never reached the preset detection limit of 2 $\log_{10}$ CFU/g. DAP alone at 6 mg/kg caused a modest CFU reduction within 8 h of exposure (−Δ 2 $\log_{10}$ CFU/g), with significant regrowth up to the initial inoculum within 72 h. DAP 8 to 12 mg/kg simulations demonstrated initial bactericidal activity but with significant regrowth to a steady-state $\log_{10}$ CFU/g of between ~6 and 7.

Both combination regimens of DAP 6 mg/kg plus CRO (2 g and 0.5 g) were superior to all DAP-alone regimens ($P < 0.001$) when tested with strain 351. These combination regimens were not superior to CRO-alone regimens, despite the MIC of this strain for CRO being 8 mg/liter ($P > 0.05$). However, the time to reduce the CFU per gram to the detection limit was delayed in comparison to that for DAP-CRO combination regimens.

For strain SF100 (Fig. 2), the SEV killing data were very similar to those for strain 351: (i) none of the DAP-alone regimens had bactericidal activity that reached the assay detection limits; (ii) both DAP plus CRO regimens were highly effective in reducing SEV counts, as was the CRO-alone regimen; and (iii) the DAP plus CRO regimens reached the detection limits more rapidly than the CRO-alone regimens.

For both strains, at 96 h of the SEV model, DAP MICs for SEV isolates for all DAP-alone regimens were 16 to 64 mg/liter (i.e., MIC increases of ≥32-fold compared to that for the parental strains). In contrast, among the DAP 6-mg/kg plus CRO combination regiments, no DAP-R isolates were observed after 96-h exposures. No DAP-R isolates were found in CRO-alone-exposed strains after 96-h exposures. CRO 2-g q12h monotherapy showed activity against both strains (reached CFU/ml detection limit), with no CRO emergence of resistance. The CRO 0.5-g single-dose day one monotherapy regimen did not reduce CFU per milliliter and resulted in the emergence of CRO resistance (MIC of >64 mg/liter) in strain SF100. No CRO resistance was observed in strain 351 for the CRO 0.5-g single-dose regimen.

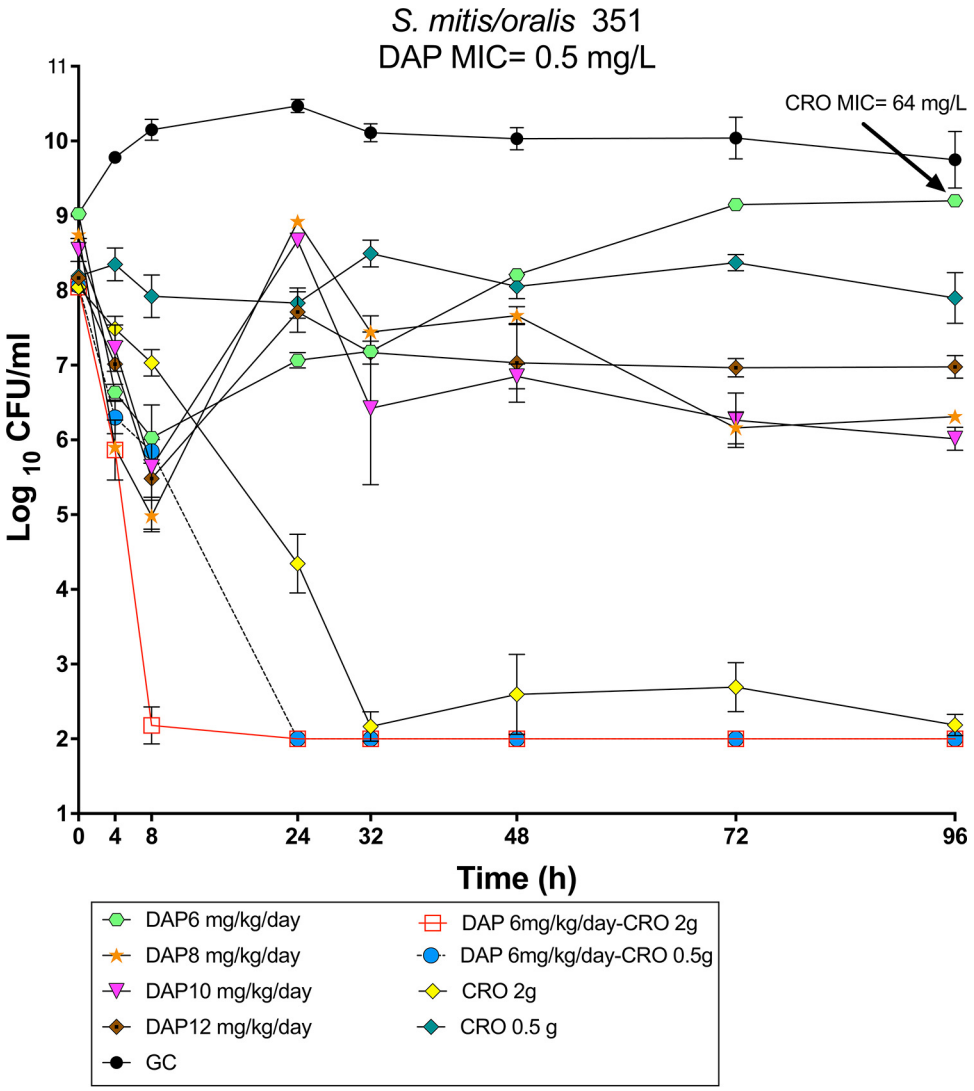

FIG 1 Comparison of daptomycin activity with and without CRO in various models in *S. mitis/oralis* 351. There was an 18-h delay in reaching the detection limit for DAP 6 mg/kg-CRO 0.5 g (single dose) in comparison to that for DAP 6 mg/kg-CRO 2 g.

Cell surface charge. Prior studies in selected *S. aureus* and enterococcal strains have shown an association between alterations in the cell surface charge toward more electropositivity and the DAP-R phenotype (27–29). In this context, we investigated the cell surface charges for both current *S. mitis/oralis* strains.

A representative 351 DAP-R SEV variant (D12T96 A1) demonstrated a significantly enhanced positive surface charge compared to its 351 DAP-S parental strain ($P < 0.05$), a phenotype observed before with this strain following derivation by serial *in vitro* DAP passage (28) (Table 3). In contrast, there was no difference in relative surface charge when comparing SF100 DAP-R (D12T96 B2) and its DAP-S parental strain.

Cytoplasmic membrane order (fluidity/rigidity). It was previously shown that there appears to be an optimal degree of cytoplasmic membrane (CM) order for maximal interaction for distinct CM-targeting cationic antimicrobial peptides, including calcium-DAP (28, 30–32). The 351 DAP-R (D12T96 A1) strain had a significantly increased CM fluidity versus its DAP-S parental strain, mirroring prior reported data for *in vitro*-derived DAP-R variants of this strain (Table 3) (28). However, there was no substantive difference of CM order in SF100 DAP-R (D12T96 B2) versus its parental strain.

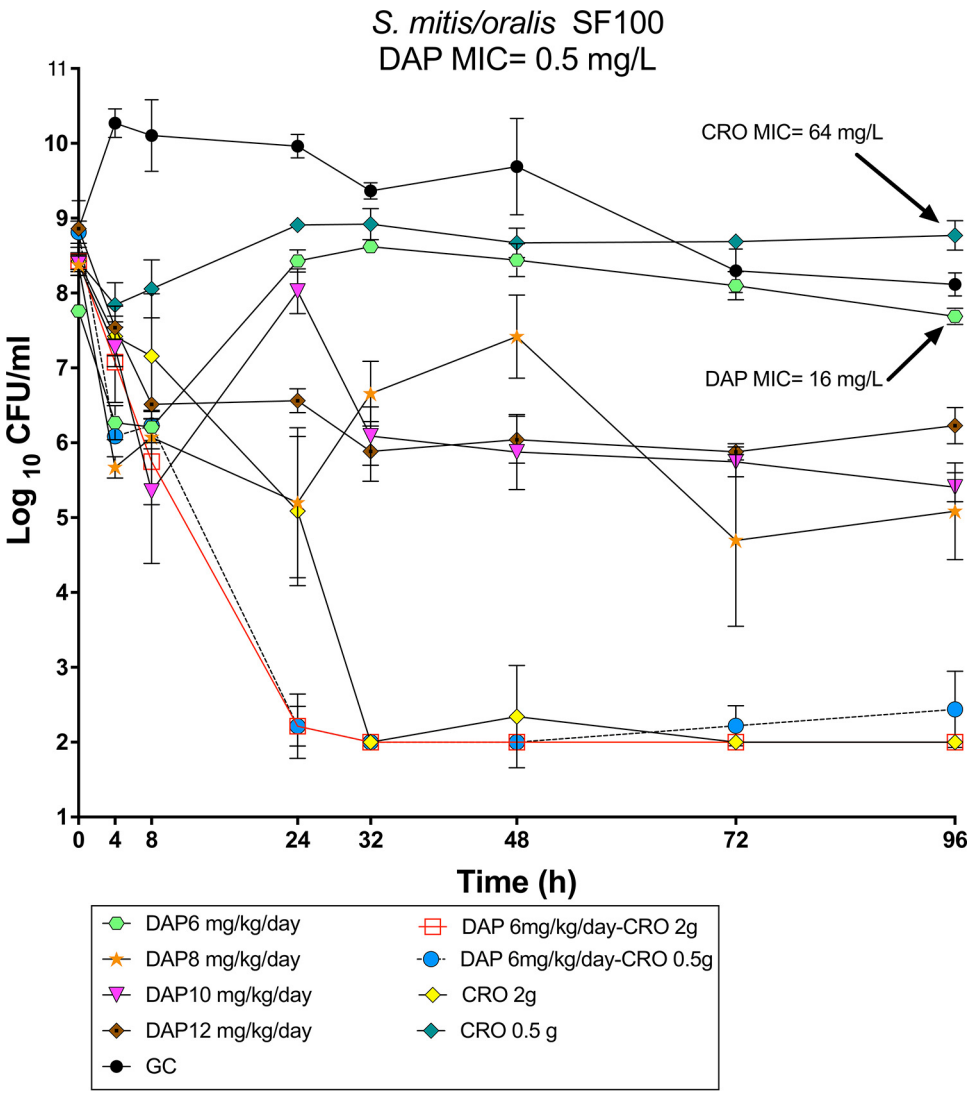

FIG 2 Comparison of daptomycin activity with and without CRO in various models in *S. mitis/oralis* SF100. DAP 6 mg/kg-CRO 0.5 g (single dose) and DAP 6 mg/kg-CRO 2 g reached the detection limit at the same time, but slight regrowth was observed in DAP 6 mg/kg-CRO 0.5 g (single dose) after 48 h.

CM phospholipid content. The CM phospholipid (PL) content is intimately involved in the mechanism of action and resistance of DAP (12, 28, 30, 32–35). As seen before (28), the 351 DAP-R (D12T96 A1) strain exhibited an apparent disappearance of both phosphatidylglycerol and cardiolipin, accompanied by a clear increase in phosphatidic acid content (the initial substrate for cardiolipin biosynthesis), compared to its DAP-S parental strain (Table 4; Fig. 3). In contrast, DAP-R SF100 (D12T96 B2) showed rather similar PL profiles to its DAP-S parental strain.

TABLE 3 Relative surface charge and CM fluidity of study strains

Strain pairs[a]	Surface charge (%)[b]	CM fluidity (PI value)
351/D12T96 A1	59 ± 9/30 ± 4[c]	0.31 ± 0.02/0.29 ± 0.03[c]
SF100/D12T96 B2	24 ± 4/25 ± 5	0.29 ± 0.00/0.30 ± 0.01

[a]First strain in each pair is the DAP-S parental strain, and the second one is the DAP-R strain.
[b]Percentage of bacterial-bound Cyt C calculated from the proportion of unbound Cyt C remaining in the supernatant.
[c]*P* value of <0.05 in 351 DAP-R (D12T96 A1) versus 351 DAP-S *S. mitis/oralis* parental strain.

TABLE 4 CM phospholipid composition of study strains

Strain pairs[a]	% of total PLs (mean ± SD)[b]		
	PG	CL	PA
351/D12T96 A1	11 ± 15/0 ± 0[c]	85 ± 16/0 ± 0[c]	4 ± 2/100 ± 0[c]
SF100/D12T96 B2	10 ± 6/20 ± 8	47 ± 5/69 ± 3	15 ± 7/6 ± 4

[a]First strain in each pair is the DAP-S parental strain, and the second one is the DAP-R strain.
[b]PG, phosphatidylglycerol; CL, cardiolipin; PA, phosphatidic acid.
[c]*P* value of <0.001 351 DAP-R (D12T96 A1) strain versus 351 DAP-S *S. mitis/oralis* parental strain.

Role of *cdsA* and *pgsA*. Daptomycin resistance was previously linked to mutations in *cdsA* and *pgsA*, two genes that mediate the synthesis of membrane phospholipids (28). For that reason, we compared the sequences of these genes in the DAP-S parental versus DAP-R variants of 351 and SF100. No mutations were present in the open reading frames of either *cdsA* or *pgsA* for either of the two DAP-R strains. For the DAP-R strain 351 variant, this indicated that the observed phospholipid changes are likely to be due to other genetic mechanisms impacting the cardiolipin biosynthetic pathway.

DISCUSSION

Several interesting observations emerged in these studies. First, our data demonstrate that addition of CRO to DAP improves the bactericidal activity of DAP both *ex vivo* and *in vivo* against two prototypical *S. mitis/oralis* strains and also prevents the emergence of DAP-R during prolonged DAP exposures in the SEV model. Of note, even a single exposure to low-dose CRO enhanced the bactericidal activity of DAP in this

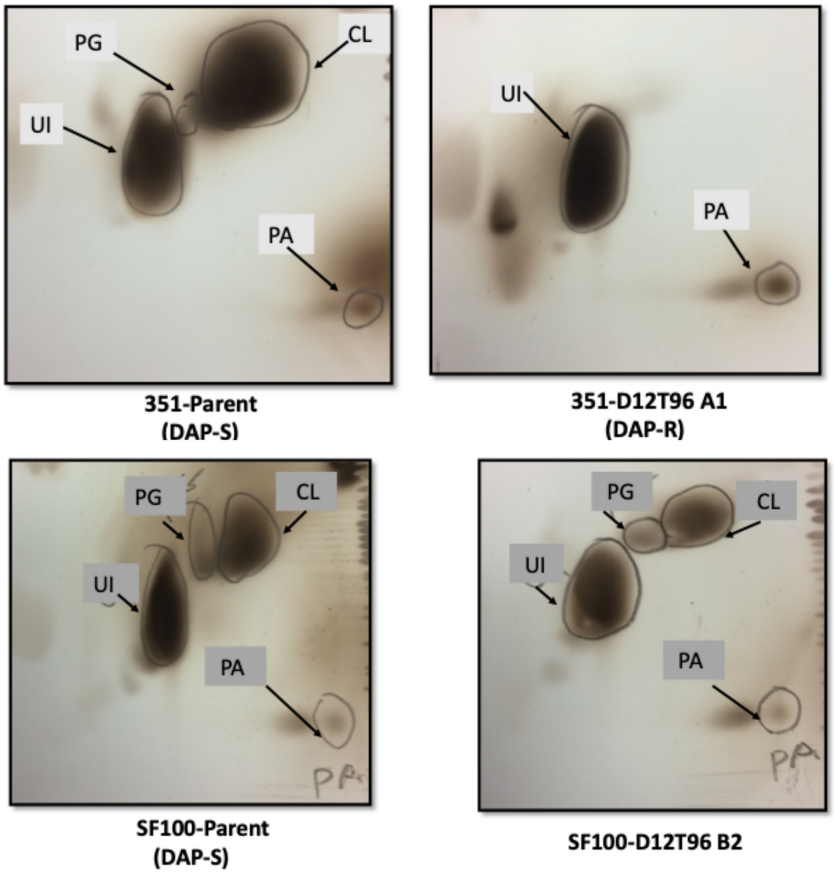

FIG 3 Phospholipid spots shown in 2D-TLC plates were developed with $CuSO_4$ (100 mg/ml) spray containing 8% phosphoric acid and heated at 180°C. PG, phosphatidylglycerol; CL, cardiolipin; PA, phosphatidic acid; UI, unidentified; phospholipid, glycolipid contaminant seen in all *S. mitis*/oralis strains (previously detailed [29]).

model. These findings open the possibility to use this antibiotic combination for treating *S. mitis/oralis* infective endocarditis in clinical settings.

Second, we studied a range of DAP-alone simulated dose strategies (6, 8, 10, and 12 mg/kg/day) to approximate current clinical regimens for invasive Gram-positive infections (19) in hopes of overriding the propensity of *S. mitis/oralis* strains to develop DAP-R (2). Our goal was to significantly enhance DAP penetration of the SEVs and thus maximize the amount of drug reaching intra-SEV *S. mitis/oralis* colonies. We previously demonstrated that a 6-mg/kg/day human-simulated dose equivalent is able to achieve more than 60% (48.2/79.5 μg/ml) DAP penetration into the SEV (36). This would put the concentration of DAP (48 μg/ml) well above the MICs of both parenteral *S. mitis/oralis* strains used in the present paper. However, despite significant increases in C_{max} and AUC_{0-24} accompanying escalating DAP-alone dose strategies (6, 8, 10, and 12 mg/kg simulations in the SEV model), such regimens only modestly reduced bacterial burdens in SEV and were not able to prevent the evolution of high-level DAP-R in SEVs infected with either study strains. The same findings were observed in the rabbit model of *S. mitis* experimental endocarditis using 6 and 10 mg/kg of daptomycin (2).

Third, since DAP-R was previously linked to mutations in *cdsA* and/or *pgsA* (14, 28), we compared the sequences of these genes in the parental versus their respective DAP-R variants derived from SEVs after 96 h of DAP-alone exposures. Of note, and in contrast to data we have previously published for DAP-R variants of these two study strains following serial *in vitro* or *in vivo* DAP exposures in experimental IE (3), there were no SNPs found in either open reading frame (ORF) when comparing parental versus DAP-R variants. These data suggest that the evolution of DAP-R in a distinct environmental milieu (*in vitro* versus *ex vivo* versus *in vivo*) follows different genetic and/or metabolic pathway perturbations and is influenced by the unique characteristics of each microenvironment. For example, SEVs feature platelet-fibrin matrices bathed in artificial growth medium, while *in vivo* vegetations contain similar matrices in the presence of a variety of host defense cells (e.g., polymorphonuclear leukocytes [PMNs]) and molecules (e.g., antibody, complement, and host defense cationic peptides).

Fourth, for strain 351, its *ex vivo*-derived DAP-R variant featured an apparent disappearance of phosphatidylglycerol (PG) and cardiolipin (CL) accompanied by increased phosphatidic acid (PA) content; this pattern of phospholipid content is identical to that previously seen with the serial *in vitro* passage of organisms exposed to DAP alone (28). However, the SNPs in *cdsA* that accompany this phenotype in the *in vitro*-derived DAP-R 351 variant were not observed among SEV-derived DAP-R 351 variants. In aggregate, these findings indicate the above-described changes in CM phospholipids and subsequent DAP-R involve different genetic pathways. Such mutations may alter the expression of *cdsA* or *pgsA* or, alternatively, may affect membrane biogenesis via other pathways. Whole-genome sequencing comparative analyses are in progress to further adjudicate this issue.

One additional explanation for PG-CL disappearance in DAP-R strain 351, in the absence of perturbations in CL biosynthetic genes, could be an upregulation of release of these phospholipids extracellularly. This paradigm has been recently proposed by the Edwards' laboratory involving the interaction of *Staphylococcus aureus*, enterococci, and VGS of the *S. mitis* group (i.e., *S. gordonii*) with DAP (37, 38). They documented the capacity of these organisms to release such phospholipids extracellularly in an active process, which could then bind to and inactivate DAP in a "phospholipid decoy" mechanism. However, this mechanism would tend to bind DAP extracellularly and prevent its binding to target CMs; this, however, is the opposite of what has been previously observed in DAP-R *S. mitis/oralis* strains (29).

Fifth, in contrast to strain 351, no substantive changes in PL profiles were found in DAP-R SF100 variants isolated from SEVs. These outcomes support the notion that the genetic basis of the PG-CL disappearance during emergence of DAP-R in strain 351 under *ex vivo* conditions involves loci and/or pathways outside the standard CL biosynthetic schema. Moreover, these data sets point to a distinct and strain-specific

mechanism(s) of DAP-R emerging *ex vivo* in variants of SF100, not involving CL biosynthesis.

Sixth, one prevailing concept that has been put forward to explain, at least in part, the DAP-R phenotype in Gram-positive pathogens, including *S. mitis/oralis*, has been alterations in relative cell surface positive charge, creating a "charge-repulsion" milieu against calcium-DAP and other cationic peptides. Interestingly, and as seen before (28), the *in vitro*-derived DAP-R 351 variant showed a significant enhancement of positive surface charge versus its DAP-S parental strain. However, this phenotypic perturbation was not seen in the DAP-R SF100 variant. These data do not support charge repulsion as a sole or global explanation for the DAP-R phenotype in these strain pairs and further support the strain specificity of DAP-R mechanisms in *S. mitis/oralis* strains.

Lastly, in general, alterations in CM fluidity have been closely related to resistance to killing by calcium-DAP and other cationic peptides among DAP-R Gram-positive pathogens (1–8). These phenotypes are believed to link to an altered ability of DAP to interact with and/or insert within target CMs at extremes of CM order. It is presumed that there are certain CM order set points for the optimal interaction of target CMs with cationic peptides such as calcium-DAP, rendering strains more or less susceptible to such agents (1–8). The DAP-R 351 (but not the DAP-R SF100) variant demonstrated significant increases in CM fluidity compared to that of its DAP-S parental strain. The enhancement of CM fluidity in the 351 DAP-R strain may partly explain the mechanism of DAP-R evolving within SEVs *ex vivo*, but this phenotype is clearly strain specific.

In conclusion, the mechanism(s) of DAP-R in *S. mitis/oralis* emerging when the organism is growing within a platelet-fibrin *ex vivo* matrix is most likely to be multifactorial, strain specific, and distinct from those evolving during *in vitro* or *in vivo* passage, although there appear to be definite overlapping scenarios. Furthermore, it is highly probable that other compensatory adaptive metabolic changes are critically important in dictating DAP-R in *S. mitis/oralis*. Importantly, CM phenotypic perturbations may well be identifiable in specific *ex vivo*-derived DAP-R *S. mitis/oralis* strains (e.g., DAP-R 351) and correlate with signature phenotypic consequences (i.e., changes in PLs, relative surface charge, and/or CM fluidity). We recognize that one major limitation in our study is only having investigated two *S. mitis/oralis* strains, which restricts the generalizability of our data. In this regard, additional investigations that include more *S. mitis/oralis* strains and other β-lactams with various exposure regimens are in- progress in our laboratories. In addition, our SEV models were terminated after only 96 h. Thus, longer antibiotic exposure times in this SEV model should be explored in future studies to more closely mirror the *in vivo* circumstance in IE.

Notwithstanding these limitations, we have now demonstrated that *S. mitis/oralis* strains are apparently capable of developing DAP-R by more than one pathway. Moreover, given the high level of homology of *S. mitis/oralis* to other pathogenic bacterial species, it is likely that these findings are broadly applicable. In addition, the 96-h SEV model can clearly present the trend of CFU per milliliter reduction or emergence of resistance in different regimens; however, as noted above, longer antibiotic exposures with this model are warranted to determine the impact of these dosing regimens on the emergence of resistance.

MATERIALS AND METHODS

Bacterial isolates. Strains 351 and SF100 were identified to the species level previously as *S. oralis* based on whole-genome sequencing. The two respective DAP-R variants were obtained from the current SEV model following 96 h of high-dose DAP (12 mg/kg/day) simulated treatment Table 1.

Antimicrobial agents and media. DAP and CRO were obtained from Merck & Co., Inc. (Whitehouse Station, NJ). Mueller-Hinton broth II (MHB; Difco, Detroit, MI) with 50 mg/liter of calcium and 12.5 mg/liter magnesium was used for susceptibility testing. In addition, for *in vitro* susceptibility testing, the medium was supplemented with 5% lysed horse blood.

Susceptibility testing. MICs were determined in duplicates using the broth microdilution method according to the Clinical and Laboratory Standards Institute (CLSI) guidelines for viridans group streptococci (39). Combination MIC values for DAP were determined by adding in CRO at 0.5× MIC to assess the ability of CRO to reduce the DAP MIC. Daptomycin MIC fold reductions from baseline were calculated by dividing single drug DAP MICs by DAP MICs in the presence of CRO.

Surface charge. The binding profile of cytochrome *c*, a highly polycationic molecule (Cyt C), is used to mimic the interactions of cationic antimicrobial peptides, such as calcium-DAP, with charged bacterial surfaces (12, 28, 30, 32–34). This assay was used to measure the relative positive cell surface charges of our two study strains as well as their DAP-R variants emerging from the SEV model described below (12, 28, 33). Briefly, each strain was grown in brain heart infusion (BHI) medium to an optical density at 600 nm (OD_{600}) of ~1.0 and then incubated with 0.5 mg/ml of Cyt C for 10 min; the residual amount of Cyt C remaining in the bacterial supernatant was then determined spectrophotometrically (12, 28, 32, 33). An increase in the quantity of Cyt C binding (i.e., less cation in the supernate) correlates to a relatively less positively charge bacterial surface (12, 28, 30, 32, 33). These data are expressed as the mean (± standard deviation [SD]) of bound Cyt C and represent data from a minimum of four independent experiments for both strain pairs on distinct days.

CM fluidity/rigidity. Strains were grown to stationary phase at 37°C, pelleted by centrifugation, and then washed with phosphate-buffered saline (PBS). A whole-cell suspension of the study strains was assayed to quantify the degree of CM order (fluidity/rigidity) at an OD_{600} of 1.0 (~10^8 CFU ml^{-1}). The assay was performed by using and measuring the three-dimensional CM orientation of the fluorescent probe, 1,6-diphenyl-1,3,5-hexatriene (DPH) by polarizing spectrofluorimetry (excitation and emission wavelengths of 360 nm and 426 nm, respectively). The descriptive method for quantifying DPH integration into CMs and the calculations of the degree of fluorescence polarization (polarization index [PI]) are described elsewhere (28, 30, 32). An inverse relationship occurs between PI values and CM fluidity (i.e., lower PI equates to a greater extent of CM fluidity) (28, 30, 32). These data included a minimum of three independent experiments on different days.

CM PL composition. The lipid extraction procedures have been previously described elsewhere (28, 30, 32, 34). The *S. mitis/oralis* strain's major PLs, PG, CL, and PA, were separated by utilizing two-dimensional thin-layer chromatography (2D-TLC) in a unique solvent system as described before (12, 28, 30, 33, 34). All TLC plates showed a copurified glycolipid (identified as digalactosyldiacylglycerol by mass spectrometry [28]) found in all our study *S. mitis/oralis* strains to date. The well-separated PL spots were scraped from the TLC plates and digested at 180°C for 3 h with 0.3 ml 70% perchloric acid, and absorbance profiles were measured spectrophotometrically at OD_{660} to quantify the phosphorus content. The TLC plates were expose to iodine vapors and sprayed with cupric sulfate ($CuSO_4$; 100 mg/ml) containing 8% (vol/vol) phosphoric acid and heated at 180°C (12, 28, 30, 31, 34) for accurate identification and confirmation of all spots on the TLC plate.

***cdsA* and *pgsA* amplification and sequence analysis.** Genomic DNA was used for PCR amplification of *cdsA* and *pgsA*, and the amplicons were isolated from the designated *S. mitis* strains as previously described (28). Vent DNA polymerase was used for standard PCR amplification. Generated PCR products encompassing the entire open reading frame for the designated gene were purified using a Qiagen PCR purification kit and sequenced by Sequetech (Mountain View, CA). Sequence reads were assembled and aligned using CLC Sequence Viewer (CLC Bio, Aarhus, Denmark).

***Ex vivo* PK/PD model.** A well-characterized, simulated endocardial vegetation (SEV) pharmacokinetic/pharmacodynamic (PK/PD) model was used for all antibiotic experiments (40, 41). SEVs were prepared as previously described (42), by mixing cryoprecipitate as the source of fibrin, a platelet suspension (American Red Cross), aprotinin (Sigma-Aldrich), and an organism suspension (final inoculum, 10^9 CFU/0.5 g). This methodology results in SEVs that contain approximately 3 to 3.5 g/dl of albumin and 6.8 to 7.4 g/dl of total protein (42). The resultant SEV mixture was then clotted using bovine thrombin in siliconized microcentrifuge tubes (Pfizer, New York, NY, USA). SEVs were removed from the tubes and suspended in the model via a sterile monofilament line. Fresh medium was continuously added and removed from the model along with the drug via a peristaltic pump (Masterflex; Cole-Parmer Instrument Company, Chicago, IL, USA) at a rate which was set to simulate the half-lives of the antibiotics of interest. For the SEV model, due to the dependency of DAP on calcium for antimicrobial activity and calcium loss from the medium due to calcium binding to albumin, the medium was supplemented to a concentration of 75 mg/liter of calcium as previously described (23).

At assigned times, SEVs were removed from the chamber model, weighed, homogenized, and quantitatively cultured to determine *S. mitis/oralis* counts. Tryptic soy agar supplemented with 5% sheep's blood (Difco) was used for quantitative subculturing from the SEV models. Plates were incubated in an anaerobic chamber for 18 to 24 h at 37°C before performing colony counts. Bacterial counts were graphed versus time over 96 h to evaluate bactericidal activity of single and combination regimens (Fig. 1 and 2). The limit of detection for these samples is 2 $\log_{10}$ CFU/g. Results were plotted ($\log_{10}$ CFU/g versus time [h]) for determining antibacterial activity.

DAP was administered once daily via an injection port. The simulated DAP regimens with a targeted $t_{1/2}$ of 8 h were 6, 8, 10, and 12 mg/kg/day, with peak concentrations of 93.9, 123.3, 141.1, and 183.7 mg/liter, respectively. The DAP regimens were tested alone and in combination with CRO 2 g (once daily over 96 h) or 0.5 g (single dose on day one), at corresponding CRO peaks of 257 and 64.25 mg/liter, respectively. All models were performed in duplicates to ensure reproducibility.

PD analyses. For PD evaluations, two SEVs (clots) were aseptically removed from each model (total of 4 samples) at 0-, 4-, 8-, 24-, 32-, 48-, 72-, and 96-h time points. After weighing, each SEV was homogenized with trypsin, serially diluted with cold normal saline, and plated. To minimize the antibiotic carryover, the SEV samples were diluted appropriately before plating. Bactericidal and bacteriostatic activities for DAP alone or DAP-CRO combinations were defined as ≥3 $\log_{10}$ and ≤3 $\log_{10}$ CFU/g reductions in counts compared to that for untreated control SEVs. The impact of DAP-CRO combinations was defined as "enhanced" if the combination reduced SEV counts by ≥2 $\log_{10}$ CFU/g versus the

DAP-alone or CRO-alone regimens. Reductions in bacterial counts by 1 $\log_{10}$ to 2 $\log_{10}$ CFU/g compared with the most active single agent were considered "indifferent."

PK analyses. Sampling for PK assays was performed by removing 1 ml of medium (through the injection port) from each of the two parallel SEV models at 0, 2, 4, 6, 8, 24, 48, 72, and 96 h in duplicates as previously described (43). DAP PK evaluations were confirmed by a validated high-performance liquid chromatography assay that conforms to the guidelines set forth by the College of American Pathologists (44). A bioassay method was applied for assessing concentrations of CRO using *Kocuria rhizophila* (formerly known as *Micrococcus luteus*) ATCC 9341. For combination regimens, CRO concentrations were determined with *Escherichia coli* ATCC 25922 as the test organism. All assays and standards were performed in duplicates.

Sterile 0.25-in. paper disks were placed on agar (antibiotic medium 11 Difco agar plate containing 0.5 McFarland suspension of this organism). Each blank paper disk was filled with 20 μl of either a standard CRO concentration or the unknown chamber model samples from different time points (SEV PK samples). A standard curve was then created using inhibition zone size versus known concentrations; the inhibition zone sizes at each sample time point were plotted against this standard curve for the calculation of PK parameters. All samples were examined in duplicates. The CRO peak, AUC_{0-24}, and half-life metrics were determined by the trapezoidal method, utilizing standard pharmacokinetic modeling software (PK analyst version 1.1; MicroMath Scientific Software, Salt Lake City, UT).

Emergence of DAP-R in the SEV model. The emergence of DAP-R over 96-h DAP exposures within the SEV model was evaluated by determining DAP MICs of isolates recovered from 96-h SEVs when parallel plated on antibiotic-free and DAP-containing plates (3× the baseline MIC of the parental DAP-S strain). The DAP MICs of colonies detected on DAP-containing plates were then formally determined using the broth microdilution technique via CLSI guidelines (39).

Statistical analysis. The two-tailed Student's *t* test was used for statistical analysis of quantitative data related to cell surface charge, fluidity, and phospholipid content. One-way analysis of variance (ANOVA) with Tukey's *post hoc* test was applied to compare PD outcomes in the SEV model regarding DAP, CRO, and DAP-CRO combination impacts upon $\log_{10}$ CFU per gram comparative results. *P* values of $\leq$0.05 were considered significant.

ACKNOWLEDGMENTS

This work was supported by NIAID R01 AI121400 to M.J.R., R01 AI134637 and K24 AI114818 to C.A.A., K08 AI113317 to T.T.T., and R01 AI130056 to A.S.B.

M.J.R. has received grant support and has been part of a speaker bureau or consulted for Allergan, Bayer, ContraFect, Melinta, Merck, and Theravance. C.A.A. has received grant support from Merck, MeMed Diagnostics, and Entasis Therapeutics. A.S.B. has current research grants with ContraFect Corporation and Intron Pharmaceuticals. J.M.M. received a personal 80:20 research grant from the Institut d'Investigacions Biomèdiques August Pi i Sunyer (IDIBAPS), Barcelona, Spain, during 2017 to 2019.

REFERENCES

1. Doern CD, Burnham CA. 2010. It's not easy being green: the viridans group streptococci, with a focus on pediatric clinical manifestations. J Clin Microbiol 48:3829–3835. https://doi.org/10.1128/JCM.01563-10.
2. Garcia-de-la-Maria C, Pericas JM, Del Rio A, Castaneda X, Vila-Farres X, Armero Y, Espinal PA, Cervera C, Soy D, Falces C, Ninot S, Almela M, Mestres CA, Gatell JM, Vila J, Moreno A, Marco F, Miro JM, Hospital Clinic Experimental Endocarditis Study Group. 2013. Early *in vitro* and *in vivo* development of high-level daptomycin resistance is common in mitis group streptococci after exposure to daptomycin. Antimicrob Agents Chemother 57:2319–2325. https://doi.org/10.1128/AAC.01921-12.
3. Garcia-de-la-Maria C, Xiong YQ, Pericas JM, Armero Y, Moreno A, Mishra NN, Rybak MJ, Tran TT, Arias CA, Sullam PM, Bayer AS, Miro JM. 2017. Impact of high-level daptomycin resistance in the *Streptococcus mitis* group on virulence and survivability during daptomycin treatment in experimental infective endocarditis. Antimicrob Agents Chemother 61: e02418-16. https://doi.org/10.1128/AAC.02418-16.
4. Rasmussen LH, Hojholt K, Dargis R, Christensen JJ, Skovgaard O, Justesen US, Rosenvinge FS, Moser C, Lukjancenko O, Rasmussen S, Nielsen XC. 2017. *In silico* assessment of virulence factors in strains of Streptococcus oralis and *Streptococcus mitis* isolated from patients with infective endocarditis. J Med Microbiol 66:1316–1323. https://doi.org/10.1099/jmm.0.000573.
5. Bek-Thomsen M, Tettelin H, Hance I, Nelson KE, Kilian M. 2008. Population diversity and dynamics of *Streptococcus mitis*, *Streptococcus oralis*, and *Streptococcus infantis* in the upper respiratory tracts of adults, determined by a nonculture strategy. Infect Immun 76:1889–1896. https://doi.org/10.1128/IAI.01511-07.
6. Smith JR, Barber KE, Raut A, Rybak MJ. 2015. Beta-lactams enhance daptomycin activity against vancomycin-resistant *Enterococcus faecalis* and *Enterococcus faecium* in *in vitro* pharmacokinetic/pharmacodynamic models. Antimicrob Agents Chemother 59:2842–2848. https://doi.org/10.1128/AAC.00053-15.
7. Barber KE, Ireland CE, Bukavyn N, Rybak MJ. 2014. Observation of "seesaw effect" with vancomycin, teicoplanin, daptomycin and ceftaroline in 150 unique MRSA strains. Infect Dis Ther 3:35–43. https://doi.org/10.1007/s40121-014-0023-0.
8. Jensen A, Valdorsson O, Frimodt-Moller N, Hollingshead S, Kilian M. 2015. Commensal streptococci serve as a reservoir for beta-lactam resistance genes in *Streptococcus pneumoniae*. Antimicrob Agents Chemother 59:3529–3540. https://doi.org/10.1128/AAC.00429-15.
9. Marron A, Carratala J, Alcaide F, Fernandez-Sevilla A, Gudiol F. 2001. High rates of resistance to cephalosporins among viridans-group streptococci causing bacteraemia in neutropenic cancer patients. J Antimicrob Chemother 47:87–91. https://doi.org/10.1093/jac/47.1.87.
10. Nakayama A, Takao A. 2003. Beta-lactam resistance in *Streptococcus mitis* isolated from saliva of healthy subjects. J Infect Chemother 9:321–327. https://doi.org/10.1007/s10156-003-0286-y.
11. Zapata B, Alvarez DN, Farah S, Garcia-de-la-Maria C, Miro JM, Sakoulas G, Bayer AS, Mishra NN. 2018. Prevention of high-level daptomycin-resistance emergence *in vitro* in *Streptococcus mitis-oralis* by using combination antimicrobial strategies. Curr Microbiol 75:1062–1067. https://doi.org/10.1007/s00284-018-1491-3.
12. Mishra NN, Yang S-J, Chen L, Muller C, Saleh-Mghir A, Kuhn S, Peschel A, Yeaman MR, Nast CC, Kreiswirth BN, Crémieux A-C, Bayer AS. 2013.

Emergence of daptomycin resistance in daptomycin-naive rabbits with methicillin-resistant *Staphylococcus aureus* prosthetic joint infection is associated with resistance to host defense cationic peptides and mprF polymorphisms. PLoS One 8:e71151. https://doi.org/10.1371/journal.pone.0071151.
13. Tran TT, Mishra NN, Seepersaud R, Diaz L, Rios R, Dinh AQ, Garcia-de-la-Maria C, Rybak MJ, Miro JM, Shelburne S, Sullam PM, Bayer AS, Arias CA. 2018. Mutations in *cdsA* and *pgsA* correlate with daptomycin resistance in *Streptococcus mitis* and *S. oralis*. Antimicrob Agents Chemother 63:e01531-18. https://doi.org/10.1128/AAC.01531-18.
14. Adams HM, Joyce LR, Guan Z, Akins RL, Palmer KL. 2017. *Streptococcus mitis* and *S. oralis* lack a requirement for CdsA, the enzyme required for synthesis of major membrane phospholipids in bacteria. Antimicrob Agents Chemother 61:e02552-16. https://doi.org/10.1128/AAC.02552-16.
15. Bensing BA, Rubens CE, Sullam PM. 2001. Genetic loci of *Streptococcus mitis* that mediate binding to human platelets. Infect Immun 69:1373–1380. https://doi.org/10.1128/IAI.69.3.1373-1380.2001.
16. Miller WR, Bayer AS, Arias CA. 2016. Mechanism of action and resistance to daptomycin in *Staphylococcus aureus* and enterococci. Cold Spring Harb Perspect Med 6:a026997. https://doi.org/10.1101/cshperspect.a026997.
17. Davlieva M, Zhang W, Arias CA, Shamoo Y. 2013. Biochemical characterization of cardiolipin synthase mutations associated with daptomycin resistance in enterococci. Antimicrob Agents Chemother 57:289–296. https://doi.org/10.1128/AAC.01743-12.
18. Zhang T, Muraih JK, Tishbi N, Herskowitz J, Victor RL, Silverman J, Uwumarenogie S, Taylor SD, Palmer M, Mintzer E. 2014. Cardiolipin prevents membrane translocation and permeabilization by daptomycin. J Biol Chem 289:11584–11591. https://doi.org/10.1074/jbc.M114.554444.
19. Yim J, Smith JR, Singh NB, Rice S, Stamper K, Garcia de la Maria C, Bayer AS, Mishra NN, Miro JM, Tran TT, Arias CA, Sullam P, Rybak MJ. 2017. Evaluation of daptomycin combinations with cephalosporins or gentamicin against *Streptococcus mitis* group strains in an in vitro model of simulated endocardial vegetations (SEVs). J Antimicrob Chemother 72:2290–2296. https://doi.org/10.1093/jac/dkx130.
20. Kebriaei R, Rice SA, Singh KV, Stamper KC, Dinh AQ, Rios R, Diaz L, Murray BE, Munita JM, Tran TT, Arias CA, Rybak MJ. 2018. Efficacy of daptomycin monotherapy and in combination with beta-lactams for daptomycin-susceptible *Enterococcus faecium* harboring LiaSR substitutions: influence of the inoculum effect. Antimicrob Agents Chemother 62:e00315-18. https://doi.org/10.1128/AAC.00315-18.
21. Smith DL, Singh KV, Tran TT, Arias CA, Murray BE. 2016. Daptomycin plus ceftaroline against daptomycin-resistant *Enterococcus faecium* in a rat model of experimental endocarditi. Open Forum Infect Dis 3 Suppl 1:1980.
22. Smith JR, Barber KE, Raut A, Aboutaleb M, Sakoulas G, Rybak MJ. 2015. Beta-lactam combinations with daptomycin provide synergy against vancomycin-resistant *Enterococcus faecalis* and *Enterococcus faecium*. J Antimicrob Chemother 70:1738–1743. https://doi.org/10.1093/jac/dkv007.
23. Steed ME, Vidaillac C, Rybak MJ. 2010. Novel daptomycin combinations against daptomycin-nonsusceptible methicillin-resistant *Staphylococcus aureus* in an *in vitro* model of simulated endocardial vegetations. Antimicrob Agents Chemother 54:5187–5192. https://doi.org/10.1128/AAC.00536-10.
24. Akins RL, Katz BD, Monahan C, Alexander D. 2015. Characterization of high-level daptomycin resistance in viridans group streptococci developed upon *in vitro* exposure to daptomycin. Antimicrob Agents Chemother 59:2102–2112. https://doi.org/10.1128/AAC.04219-14.
25. Sader HS, Flamm RK, Farrell DJ, Jones RN. 2013. Daptomycin activity against uncommonly isolated streptococcal and other Gram-positive species groups. Antimicrob Agents Chemother 57:6378–6380. https://doi.org/10.1128/AAC.01906-13.
26. Liu C, Bayer A, Cosgrove SE, Daum RS, Fridkin SK, Gorwitz RJ, Kaplan SL, Karchmer AW, Levine DP, Murray BE, Rybak MJ, Talan DA, Chambers HF. 2011. Clinical practice guidelines by the Infectious Diseases Society of America for the treatment of methicillin-resistant *Staphylococcus aureus* infections in adults and children: executive summary. Clin Infect Dis 52:285–292. https://doi.org/10.1093/cid/cir034.
27. Mishra NN, Yang SJ, Sawa A, Rubio A, Nast CC, Yeaman MR, Bayer AS. 2009. Analysis of cell membrane characteristics of *in vitro*-selected daptomycin-resistant strains of methicillin-resistant *Staphylococcus aureus*. Antimicrob Agents Chemother 53:2312–2318. https://doi.org/10.1128/AAC.01682-08.
28. Mishra NN, Tran TT, Seepersaud R, Garcia-de-la-Maria C, Faull K, Yoon A, Proctor R, Miro JM, Rybak MJ, Bayer AS, Arias CA, Sullam PM. 2017. Perturbations of phosphatidate cytidylyltransferase (CdsA) mediate daptomycin resistance in *Streptococcus mitis/oralis* by a novel mechanism. Antimicrob Agents Chemother 61:e02435-16. https://doi.org/10.1128/AAC.02435-16.
29. Wilson WW, Wade MM, Holman SC, Champlin FR. 2001. Status of methods for assessing bacterial cell surface charge properties based on zeta potential measurements. J Microbiol Methods 43:153–164. https://doi.org/10.1016/S0167-7012(00)00224-4.
30. Mishra NN, Bayer AS, Tran TT, Shamoo Y, Mileykovskaya E, Dowhan W, Guan Z, Arias CA. 2012. Daptomycin resistance in enterococci is associated with distinct alterations of cell membrane phospholipid content. PLoS One 7:e43958. https://doi.org/10.1371/journal.pone.0043958.
31. Tsai M, Ohniwa RL, Kato Y, Takeshita SL, Ohta T, Saito S, Hayashi H, Morikawa K. 2011. *Staphylococcus aureus* requires cardiolipin for survival under conditions of high salinity. BMC Microbiol 11:13. https://doi.org/10.1186/1471-2180-11-13.
32. Mishra NN, McKinnell J, Yeaman MR, Rubio A, Nast CC, Chen L, Kreiswirth BN, Bayer AS. 2011. *In vitro* cross-resistance to daptomycin and host defense cationic antimicrobial peptides in clinical methicillin-resistant *Staphylococcus aureus* isolates. Antimicrob Agents Chemother 55:4012–4018. https://doi.org/10.1128/AAC.00223-11.
33. Mishra NN, Bayer AS, Weidenmaier C, Grau T, Wanner S, Stefani S, Cafiso V, Bertuccio T, Yeaman MR, Nast CC, Yang SJ. 2014. Phenotypic and genotypic characterization of daptomycin-resistant methicillin-resistant *Staphylococcus aureus* strains: relative roles of mprF and dlt operons. PLoS One 9:e107426. https://doi.org/10.1371/journal.pone.0107426.
34. Mishra NN, Bayer AS. 2013. Correlation of cell membrane lipid profiles with daptomycin resistance in methicillin-resistant *Staphylococcus aureus*. Antimicrob Agents Chemother 57:1082–1085. https://doi.org/10.1128/AAC.02182-12.
35. Muller A, Wenzel M, Strahl H, Grein F, Saaki TN, Kohl B, Siersma T, Bandow JE, Sahl HG, Schneider T, Hamoen LW. 2016. Daptomycin inhibits cell envelope synthesis by interfering with fluid membrane microdomains. Proc Natl Acad Sci U S A 113:E7077–E7086. https://doi.org/10.1073/pnas.1611173113.
36. LaPlante KL, Rybak MJ. 2004. Impact of high-inoculum *Staphylococcus aureus* on the activities of nafcillin, vancomycin, linezolid, and daptomycin, alone and in combination with gentamicin, in an *in vitro* pharmacodynamic model. Antimicrob Agents Chemother 48:4665–4672. https://doi.org/10.1128/AAC.48.12.4665-4672.2004.
37. Ledger EVK, Pader V, Edwards AM. 2017. *Enterococcus faecalis* and pathogenic streptococci inactivate daptomycin by releasing phospholipids. Microbiology 163:1502–1508. https://doi.org/10.1099/mic.0.000529.
38. Pader V, Hakim S, Painter KL, Wigneshweraraj S, Clarke TB, Edwards AM. 2016. *Staphylococcus aureus* inactivates daptomycin by releasing membrane phospholipids. Nat Microbiol 2:16194. https://doi.org/10.1038/nmicrobiol.2016.194.
39. CLSI. 2018. Performance standards for antimicrobial susceptibility testing; 38th informational supplement. MS100-S38. Clinical and Laboratory Standards Institute, Wayne, PA.
40. Hall AD, Steed ME, Arias CA, Murray BE, Rybak MJ. 2012. Evaluation of standard- and high-dose daptomycin versus linezolid against vancomycin-resistant *Enterococcus* isolates in an *in vitro* pharmacokinetic/pharmacodynamic model with simulated endocardial vegetations. Antimicrob Agents Chemother 56:3174–3180. https://doi.org/10.1128/AAC.06439-11.
41. Hershberger E, Coyle EA, Kaatz GW, Zervos MJ, Rybak MJ. 2000. Comparison of a rabbit model of bacterial endocarditis and an *in vitro* infection model with simulated endocardial vegetations. Antimicrob Agents Chemother 44:1921–1924. https://doi.org/10.1128/AAC.44.7.1921-1924.2000.
42. Cha R, Rybak MJ. 2003. Daptomycin against multiple drug-resistant staphylococcus and enterococcus isolates in an *in vitro* pharmacodynamic model with simulated endocardial vegetations. Diagn Microbiol Infect Dis 47:539–546. https://doi.org/10.1016/S0732-8893(03)00119-6.
43. Hall Snyder A, Werth BJ, Barber KE, Sakoulas G, Rybak MJ. 2014. Evaluation of the novel combination of daptomycin plus ceftriaxone against vancomycin-resistant enterococci in an *in vitro* pharmacokinetic/pharmacodynamic simulated endocardial vegetation model. J Antimicrob Chemother 69:2148–2154. https://doi.org/10.1093/jac/dku113.
44. Polillo M, Tascini C, Lastella M, Malacarne P, Ciofi L, Viaggi B, Bocci G, Menichetti F, Danesi R, Del Tacca M, Di Paolo A. 2010. A rapid high-performance liquid chromatography method to measure linezolid and daptomycin concentrations in human plasma. Ther Drug Monit 32:200–205. https://doi.org/10.1097/FTD.0b013e3181d3f5cb.